Supramolecular Chemistry
Publication details, including instructions for authors and subscription information:
http://www.informaworld.com/smpp/title~content=t713649759

Inclusion Compounds Formed from *N,N*-bis(2-hydroxybenzyl)alkylamine Derivatives and Transition Metal Ions via Molecular Assembly

Suttinun Phongtamrug[a]; Buncha Pulpoka[b]; Suwabun Chirachanchai[a]
[a] The Petroleum and Petrochemical College, Chulalongkorn University, Bangkok, Thailand [b] Department of Chemistry, Faculty of Science, Chulalongkorn University, Bangkok, Thailand

To cite this Article Phongtamrug, Suttinun , Pulpoka, Buncha and Chirachanchai, Suwabun(2004) 'Inclusion Compounds Formed from *N,N*-bis(2-hydroxybenzyl)alkylamine Derivatives and Transition Metal Ions via Molecular Assembly', Supramolecular Chemistry, 16: 4, 269 — 278
To link to this Article: DOI: 10.1080/1061027042000204029
URL: http://dx.doi.org/10.1080/1061027042000204029

Supramolecular Chemistry, June 2004, Vol. 16 (4), pp. 269–278

Taylor & Francis
Taylor & Francis Group

Inclusion Compounds Formed from *N*,*N*-bis(2-hydroxybenzyl)alkylamine Derivatives and Transition Metal Ions via Molecular Assembly

SUTTINUN PHONGTAMRUG[a], BUNCHA PULPOKA[b] and SUWABUN CHIRACHANCHAI[a,*]

[a]*The Petroleum and Petrochemical College, Chulalongkorn University, Bangkok 10330, Thailand;* [b]*Department of Chemistry, Faculty of Science, Chulalongkorn University, Bangkok 10330, Thailand*

Received (in Southampton, UK) 2 October 2003; Accepted 26 January 2004

A series of *N*,*N*-bis(2-hydroxybenzyl)alkylamine derivatives (1–5) have been found to form host–guest compounds with transition metal ions. The inclusion phenomena in solution are confirmed from the new peak at 415 nm observed by UV-Vis (ultraviolet-visible) spectroscopy and the aromatic and methylene peak shifts observed by ^{1}H NMR (proton nuclear magnetic resonance) spectroscopy. Comparative studies on 1–5 by liquid–liquid extraction studies suggest that the bulky group at the aza position of the derivatives obstructs the ion interaction resulting in the decrease in ion extraction ability. Inclusion depends on the interaction of the transition metal ions with the compounds 1–5 at the aza and hydroxyl groups as identified by the two-dimensional nuclear Overhauser enhancement technique (^{1}H–^{1}H NOESY). The results from Job's plot and electrospray ionization mass spectroscopy (ESIMS) imply molecular assembly of the host–guest system in a 2:1 ratio. Comparative studies among different ions, i.e., Cu^{2+}, Zn^{2+} and Cd^{2+} suggest that the host–guest formation is effective when electron sharing is possible through the outer orbital of the transition metal ions. In the case of inclusion in the solid state, the FTIR (Fourier transform infrared) spectra show the changes in vibrational mode of the functional groups in host molecules whereas the X-ray diffraction (XRD) patterns suggest a change in the packing structure of the host molecules. After host–guest formation, the thermal stability of the host molecules decreases as a result of the change in the packing structure from a hydrogen-bonded network to one of ionic interaction with the guest.

Keywords: Inclusion; Molecular assembly; *N*,*N*′-bis(2-hydroxybenzyl)alkylamine derivatives; Transition metal ions; Hydrogen bond network; Ionic interaction

INTRODUCTION

For the past few decades, supramolecular chemistry has received much attention with regard to molecular recognition and inclusion [1–5]. With the advance of instrumentation technology, not only cyclic but also acyclic compounds can be involved in host–guest relationships based on non-covalent interactions such as van der Waals [6], dipole–dipole [7], π–π stacking [8] and hydrogen bonding [9]. Many strategies for obtaining supramolecular compounds are challenging from the fundamental molecular designs to synthesis pathways.

Polybenzoxazines are reported as a novel type of phenolic resin with superb mechanical and thermal properties, which make them suitable composite materials [10]. The structure of the repeat unit of polybenzoxazines, the aza-methylene-phenol group, resembles the aza-methylene linkage in azacalixarenes (Scheme 1) [11]. Previously, we reported the conditions for a one-step ring opening reaction of benzoxazine to quantitatively (~90% yield) obtain *N*,*N*-bis(2-hydroxybenzyl)alkylamine derivatives (Scheme 2) [12]. The structural characterization of the derivatives by single crystal X-ray analysis, NMR, and FTIR proved that the compounds are stabilized by an intra- and intermolecular hydrogen bond network [13]. Considering the uniqueness of *N*,*N*-bis(2-hydroxybenzyl)alkylamine derivatives, it is important to note that the molecule can be a basic unit for a series of macrocyclic compounds. For example, we succeeded in using this compound

*Corresponding author. Tel.: +66-2218-4134. Fax: +66-2215-4459. E-mail: csuwabun@chula.ac.th

ISSN 1061-0278 print/ISSN 1029-0478 online © 2004 Taylor & Francis Ltd
DOI: 10.1080/1061027042000204029

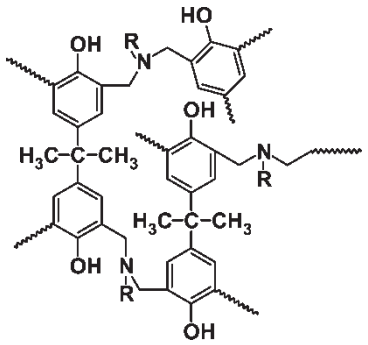

SCHEME 1

in the synthesis of a variety of macrocycles and established their inclusion phenomena with alkali and alkaline earth metal ions [14–16].

In order to extend their use to organometallic catalysis, the metal ions in the host–metal compounds need to be transition metals. Thus, another practical application for the *N,N*-bis(2-hydroxybenzyl) alkylamine derivatives would be in the generation of inclusion compounds with transition metal ions, and we expected that the electron rich phenol and aza groups might interact with transition metals. The present work thus aims to clarify (i) whether the *N,N*-bis(2-hydroxybenzyl)alkylamine derivatives exhibit inclusion phenomena with the transition metal ions, and what the host–guest ratio is, (ii) how the functional group of the derivatives plays a role in the interaction with transition metal ions, (iii) the effect of inclusion on the thermal stability of the derivatives, and (iv) the effect of solvent molecules in the host–guest system.

RESULTS AND DISCUSSION

Inclusion Phenomena of *N,N*-bis-(2-hydroxybenzyl)alkylamine Derivatives and Transition Metal Ions

In order to identify whether a host–guest compound between *N,N*-bis(2-hydroxybenzyl)alkylamine derivatives and various transition metal ions is formed, UV-Vis spectra were obtained to check for peak shift or the new peak generation. Makarska *et al.* reported that porphyrins with copper ions show inclusion phenomena as identified from the peak shifts in UV-Vis spectra [17]. Fig. 1(A) shows UV-Vis spectra of the solution **1** with $CuCl_2$ in methanol for various ratios. Compound **1** gives a peak maximum at 284 nm whereas $CuCl_2$ gives a peak at 267 nm. After mixing, a new peak at 415 nm is observed implying that **1** forms an inclusion compound with $CuCl_2$. Similarly, **2**–**4** with $CuCl_2$ gave a new peak at 415 nm, whereas **5** gave a new peak at 435 nm, confirming that *N,N*-bis(2-hydroxybenzyl)alkylamine derivatives act as hosts. Fig. 1(B) was re-plotted from Fig. 1(A) to represent the optimal host–guest ratio for **1** with $CuCl_2$. The Job's plot obtained from the new peak at 415 or 435 nm indicates that the *N,N*-bis(2-hydroxybenzyl)alkylamine derivatives (**1**–**5**) incorporate the Cu^{2+} guest in the host–guest ratio of 2:1.

^{1}H NMR was applied to study the interaction between host–metal ion and the effect of the metal ion. In order to avoid complicated conditions, methanol was selected as a good solvent for both *N,N*-bis(2-hydroxybenzyl)alkylamine derivatives and transition metal chloride salts. As shown in Fig. 2, in the case of **1**, when $CuCl_2$ was added into the system, the peak at 3.636 (–C**H**$_2$–N) ppm is significantly shifted and splits into two broad peaks at 4.118 and 4.310 ppm. The peak of C**H**$_3$–N is also substantially deshielded by 0.481 ppm. The shifting and splitting of these specific peaks imply that the proton environment at the aza and methylene groups has changed. It can be speculated that the metal ion withdraws electrons from the aza and methylene groups resulting in a decrease in electron density of these protons in the host–guest system. It was found that the other derivatives (**2**–**5**) gave the similar results suggesting host–guest formation via interaction through the aza and methylene groups.

Up to now, most reports on inclusion phenomena are for macrocyclic host compounds.

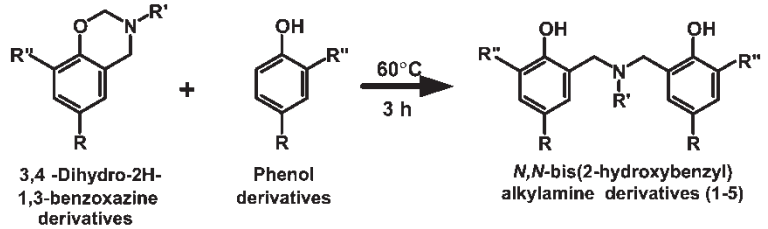

1: R= CH_3, R'= CH_3, R"= H
2: R= CH_3, R'= C_3H_7, R"= H
3: R= CH_3, R'= C_6H_{11}, R"= H
4: R= C_2H_5, R'= CH_3, R"= H
5: R= CH_3, R'= CH_3, R"= CH_3

SCHEME 2

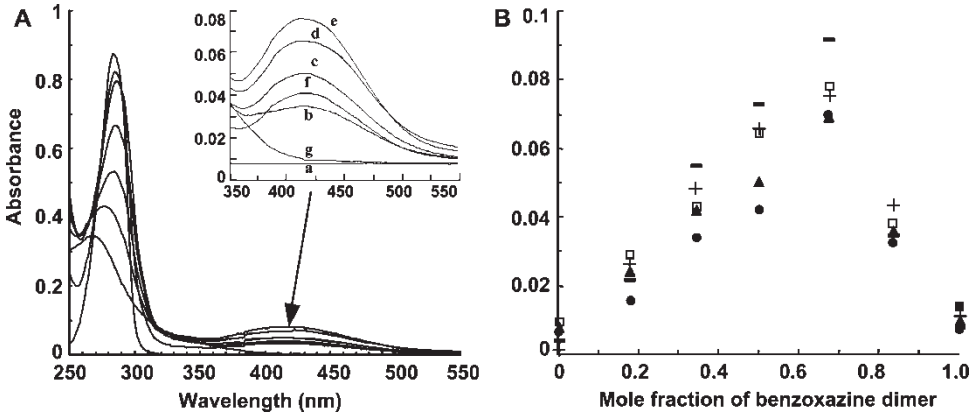

FIGURE 1 (A) UV-Vis spectra of **1**–$CuCl_2$ in methanol at various volumetric ratios; a) 0:6, b) 1:5, c) 2:4, d) 3:3, e) 4:2, f) 5:1, and g) 6:0. (B) Job's Plot as a function of mole fraction of (□) **1**, (+) **2**, (●) **3**, (−) **4** at 415 nm, and (▲) **5** at 435 nm.

However, there are cases where oligomers and small molecules can also form inclusion compounds by molecular assembly as seen in pseudocalixarenes [18], oligobenzoxazine [11] and cholic acid [19]. Ganem *et al.* demonstrated that ESIMS provide important information on the host–guest complexation of macrolides [20]. A number of host–guest molecular assembly compounds, either cyclic or noncyclic, especially calixarenes and β-cyclodextrins, were also elucidated by ESIMS [21–23]. Here, we applied ESIMS to determine how *N,N*-bis(2-hydroxybenzyl)alkylamine derivatives accept transition metal ions.

Compound **4** gives the peak (M + H) at $m/z \sim 300$ which is equal to its molecular weight (Fig. 3(a)). Moreover, a series of peaks appear at the $m/z = 300$, 600, and 899 implying that **4** tends to form an assembly structure of two and three molecules. This might be related to the inter- and intramolecular hydrogen-bond network in the solution state. The hydrogen bonding of the host structure in solution might resemble that in the solid state [13]. After complexation, the spectrum shows m/z peaks in the range of 300–370, 590–670, 890–970, 1180–1260, and 1490–1560 (Fig. 3(b)). It is important to point out that these values are close to the total of m/z of **4** and Cu^{2+}. This implies that in solution, **4** interacts with $CuCl_2$ as clusters in the host–guest ratios of $1:1 \sim 5:1$, which is significantly different from the results in Fig. 1 where the host–guest ratio for each compound in solution observed by UV-Vis was 2:1. The difference might arise from the rapid solvent evaporation *in vacuo* during ESIMS characterization.

Ion Extraction Ability of *N,N*-bis-(2-hydroxybenzyl)alkylamine Derivatives

To evaluate the efficiency of metal ion interaction, liquid–liquid extraction containing aqueous metal ions and *N,N*-bis(2-hydroxybenzyl)alkylamine derivatives dissolved in chloroform was studied. In general, the extraction percentages refer to the equilibrium between host and metal in the form of complex and free molecules existing in the solution.

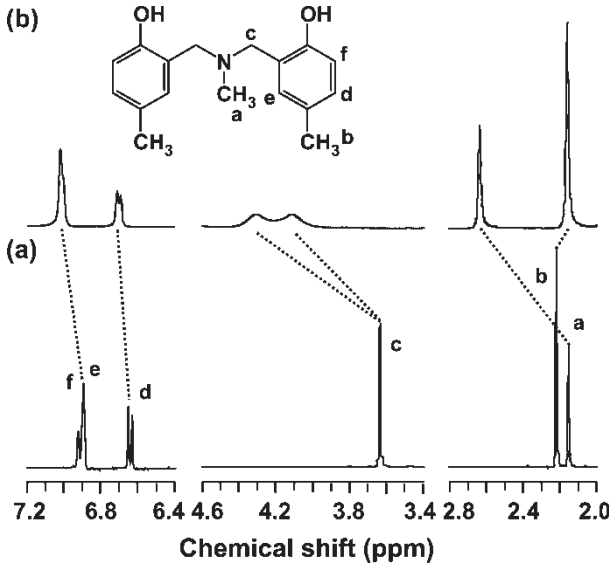

FIGURE 2 ^{1}H NMR spectra of (a) **1** and (b) **1**–$CuCl_2$ in methanol-d_4 with a 1:1 host–guest ratio.

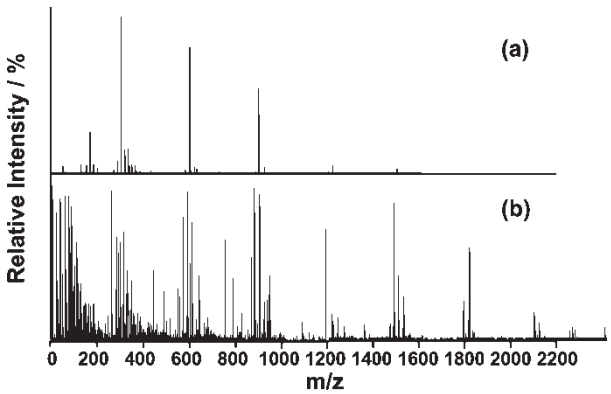

FIGURE 3 ESIMS spectra of (a) **4** and (b) **4**–$CuCl_2$ with an orifice of 35 V.

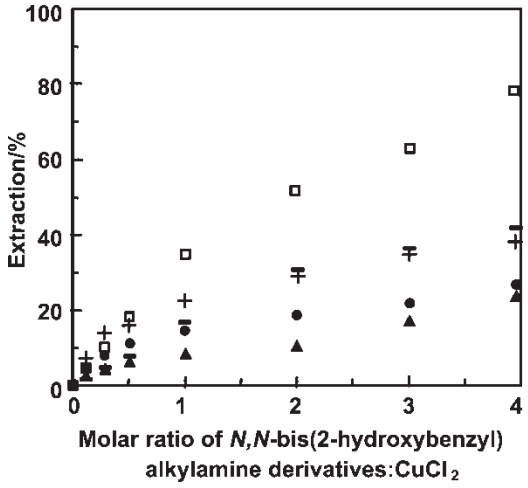

FIGURE 4 Extraction percentages of (□) **1**, (+) **2**, (●) **3**, (−) **4**, and (▲) **5** as a function of molar ratio to $CuCl_2$.

Among **1**–**5**, **1** gives the highest extraction percentage (up to 80%) whereas **5** gives the lowest (24%) (Fig. 4). In addition, the extractions of **2**–**5** are less than that of **1** (between 50% and 70% at all ratios). Here, the differences in extraction percentage might be due either to the electrical effect or the bulkiness of substituted groups. Considering the substituent group at the phenol ring, although the ethyl group donates electrons to the phenol ring, the ion extraction of **4** was not higher than that of **1** as would be expected. It should be noted that when substituent group adjacent to the nitrogen atom is a propyl or cyclohexyl group as in **2** and **3**, the extraction percentages decreased remarkably compared to **1**. Here, the bulkiness must be affecting the suitability of the *N*,*N*-bis(2-hydroxybenzyl)alkylamine derivatives for ion extraction. As seen in **1**–**5**, an increase in bulkiness at the aza group leads to a decrease in ion extraction. We speculate that the bulky group might occupy the space and obstruct the metal in interacting with the host molecule. At present, we are studying the crystal structure to confirm our speculation.

Inclusion Compounds Formed between *N*,*N*-bis-(2-hydroxybenzyl)alkylamine Derivatives and Transition Metals in the Solid State

It is important to clarify the solid state of inclusion compounds as this leads to the understanding of host–guest interactions without the solvent effect. Here, the solid state of the host–guest complex was prepared and the host–guest ratio was confirmed to be 2:1. The FTIR and XRD techniques were used to identify the changes in vibrational mode of the functional group in the host molecule and the packing structure. Spectra were recorded in Nujol in order to observe the host–guest formation with the least disturbance by moisture and water molecules.

Fig. 5 shows the FTIR spectra of **1**, **3**, and **4** before and after inclusion with $CuCl_2$ compared to the Nujol reference spectrum. In all inclusions with $CuCl_2$, a trace amount of OH is observed suggesting a weak intermolecular hydrogen bond among the host molecules. The doublet peaks at 1617 and 1597 cm^{-1} resulting from the stretching mode of C═C in the aromatic ring become a singlet implying an effect from the metal ion. The other peaks, especially, 1249 (C–N) and 1207 cm^{-1} (C–N–C) due to the aza-methylene group, become insignificant reflecting that the vibration of the functional group might be obstructed by interaction with the metal ion.

To our surprise, in the case of **3**, there was little change in FTIR spectra after complexation. This suggests that the structure of **3** might have some limitations in rearranging to accept metal guests. We speculate that there might be two types of the structure when compounds **1**–**5** encounter the metal ion, i.e., one in which metal ion interaction occurs through the hydroxyl group of the phenol unit and the aza-methylene group (the cases of **1**, **2** and **4**) and one with very weak interaction (the case of **3** and **5**). This is also relevant to the liquid–liquid extraction studies, where **3** and **5** gave lower extraction percentages than the others (Fig. 4). It is important to note that Fig. 1 shows 2:1 complex formation for **3** or **5** whereas Fig. 4 demonstrates their low extraction ability. This implies a solvent effect, which favors the complexation of **3** and **5** in methanol (Fig. 1). In other words, when the solvent is evaporated, it is difficult to maintain the host–guest interaction in solid state (Fig. 4).

The X-ray diffraction patterns indicate the packing structures and support the FTIR results. For example, the XRD pattern of **1**–$CuCl_2$ (Fig. 6(c)) is drastically changed compared to that of **1** (Fig. 6(a)), whereas the pattern of **3**–$CuCl_2$ (Fig. 6(e)) is similar to that of **3** (Fig. 6(d)). In the case of **1**–$CuCl_2$, the compound gives a series of new peaks around $2\theta = 5$–$8°$, especially at 5.58, 6.36 and 6.98° with little changes at 11–30°. This suggests that copper ions are aligned in the packing structure of **1**. For **3**–$CuCl_2$, the results from extraction percentages and the FTIR, all suggest an unchanged packing structure of the host (Fig. 6(d) and (e)).

Stability of *N*,*N*-bis(2-hydroxybenzyl)alkylamine Derivatives in the Host–metal Compound

The thermal properties of inclusion compounds are studied to assess the effect of the guest on the thermal stability of the host molecule. Rossel *et al.* reported on studies of cyclodextrin and acyclovir inclusion compounds by TGA and DSC [24]. Here, we applied DSC to assess the stability of the *N*,*N*-bis(2-hydroxybenzyl)alkylamine derivatives

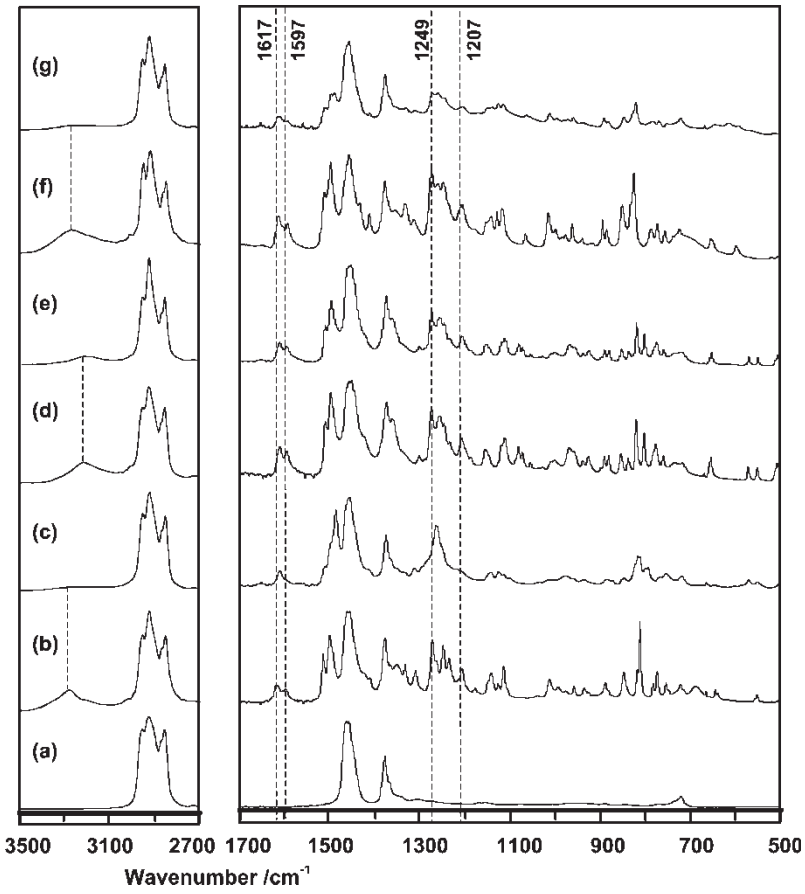

FIGURE 5 FTIR spectra of (a) Nujol, (b) **1**, (c) **1**–$CuCl_2$, (d) **3**, (e) **3**–$CuCl_2$, (f) **4** and (g) **4**–$CuCl_2$.

upon changing the hydrogen bond network after inclusion of the metal ion.

Fig. 7(a) shows that in the case of **1** with no metal guest, the melting temperature is 161°C. Here, the melting of the *N,N*-bis(2-hydroxybenzyl)alkylamine derivative reflects the stability afforded by the hydrogen-bond network as shown by the single crystal analysis [13]. However, **1**–$CuCl_2$ (2:1) shows a broad melting temperature at 130–150°C (Fig. 7(b)). This implies that the hydrogen-bond network of **1** might be obstructed after inclusion. The host–guest interactions in the solid state as evidenced from FTIR, XRD and DSC (Figs. 5–7) are relevant to those in solution shown by ^{1}H NMR (Fig. 2). We speculate that the hydrogen-bond network of **1** changes to ionic interactions with metal ions both in solution and in the solid state.

Effect of Solvent on Inclusion of *N,N*-bis-(2-hydroxybenzyl)alkylamine Derivatives

In solution, the interaction of solvent molecules may either enhance or reduce the stability and possibility of host–guest formation. In the present work, the effects of protic solvent (methanol) and aprotic solvent (DMSO and chloroform) on the inclusion compounds were observed by ^{1}H NMR. Since the host–guest ratio is 2:1 (Fig. 1), here, an excess of guest was added to the host solution in order to provide the condition that most hosts interact with guests. The $CuCl_2$ was added in deuterated solvent in an equimolar amount to the host compound.

Comparing Fig. 2 with Fig. 8, it is important to note that **1** shows an OH peak in DMSO. This implies that there are free hydroxyl groups of **1** in DMSO since the interactions in DMSO might be based on polar–polar interactions. However, after inclusion, the hydroxyl peak splits into one broad peak and one sharp peak. This suggests two structures in equilibrium, i.e., one with a hydrogen-bond network (broad peak) and one with a free hydroxyl group (sharp peak). Furthermore, the $-CH_2-N$ peak becomes broader with splitting and shifts to low field. This suggests a decrease in electron density as a result of metal ion interaction. Another significant change in the ^{1}H NMR is that two species of methyl protons appear at the same chemical shift suggesting an identical environment.

The chloroform system was also studied. After formation of the inclusion compound of **1** with $CuCl_2$ (Fig. 9(b)), the methylene protons (3.71 ppm) were slightly deshielded by 0.03 ppm. The hydroxyl

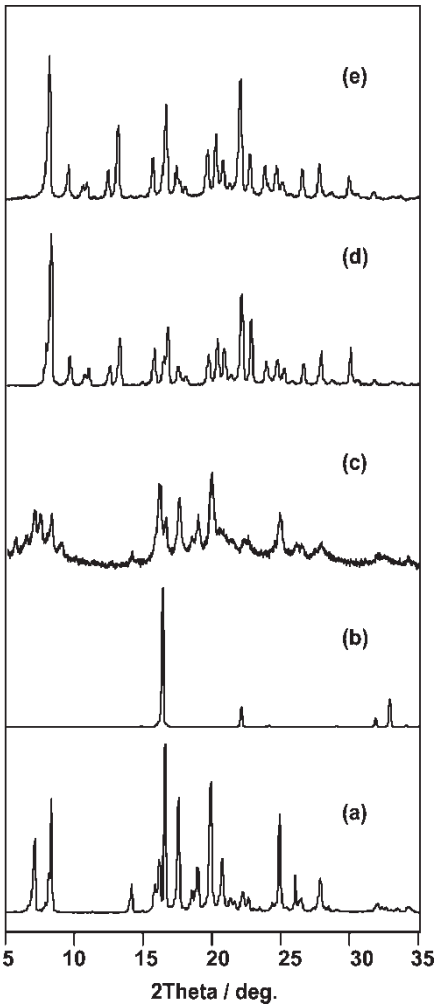

FIGURE 6 Diffraction patterns of (a) **1**, (b) $CuCl_2$, (c) **1**–$CuCl_2$, (d) **3** and (e) **3**–$CuCl_2$.

protons of **1** appearing at 9.4 ppm (Fig. 9(a)) reflect the inter and intramolecular hydrogen-bond network of **1** in $CDCl_3$. The upfield shifting of these hydroxyl protons from 9.4 to 8.2 ppm (Figure 9(b)) suggests that

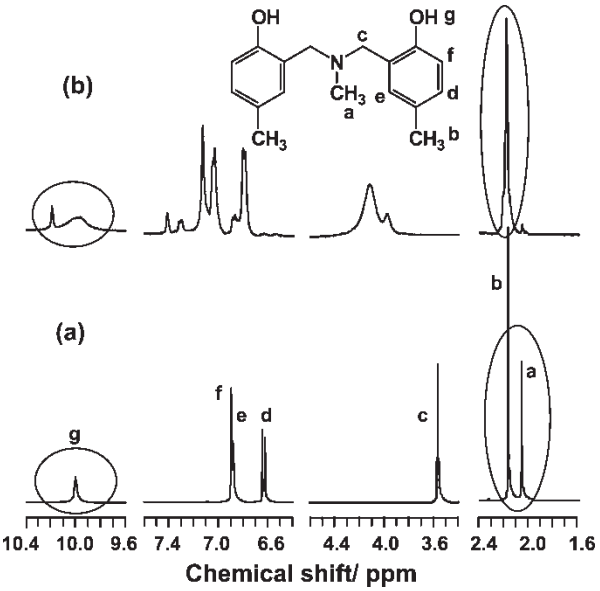

FIGURE 8 ^{1}H NMR spectra of (a) **1** and (b) **1**–$CuCl_2$ in DMSO-d_6.

when complexation occurs, the hydrogen bonding (O–H···N) might be changed to H–O···metal···N. The changes in the peaks due to the aromatic protons also support formation of an inclusion compound since those due to the phenol group are broader after complexation (Fig. 9(b)).

Here, ^{1}H–^{1}H NOESY was also carried out to obtain more information on the inclusion process [25]. Compound **1** shows the peaks involved in the interaction between protons of the hydroxyl group (H1, H2) and protons of methylene group (H7, H9) (Fig. 10(a)). In the case of **1**–$CuCl_2$ (Fig. 10(b)), the disappearance of those peaks supports our speculation about the interaction of **1** with the metal ion via the lone pair of electrons on the oxygen and nitrogen atoms. Upon inclusion, the intramolecular interaction (H1, H2 to H7, H9) decreased

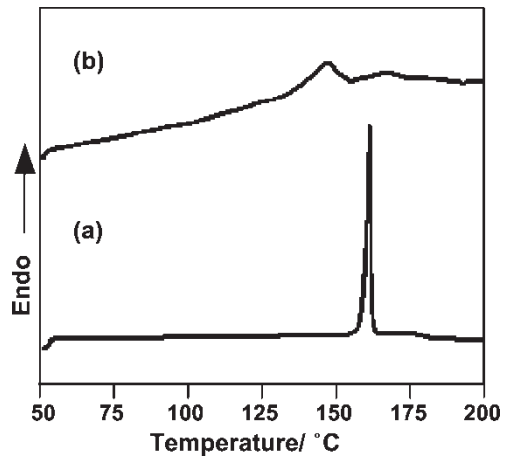

FIGURE 7 DSC thermograms of (a) **1** and (b) **1**–$CuCl_2$.

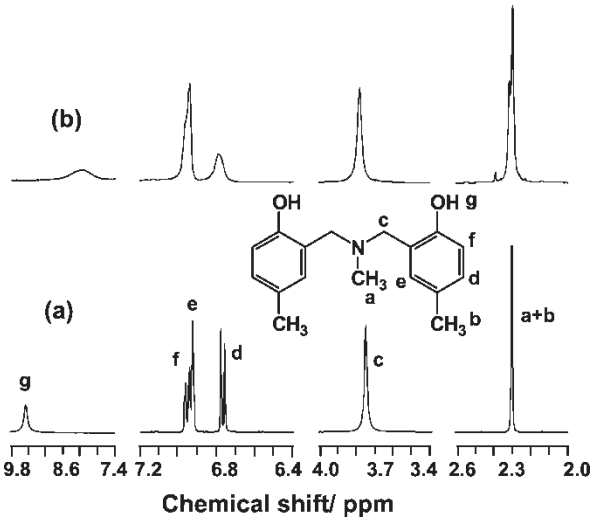

FIGURE 9 ^{1}H NMR spectra of (a) **1** and (b) **1**–$CuCl_2$ in $CDCl_3$.

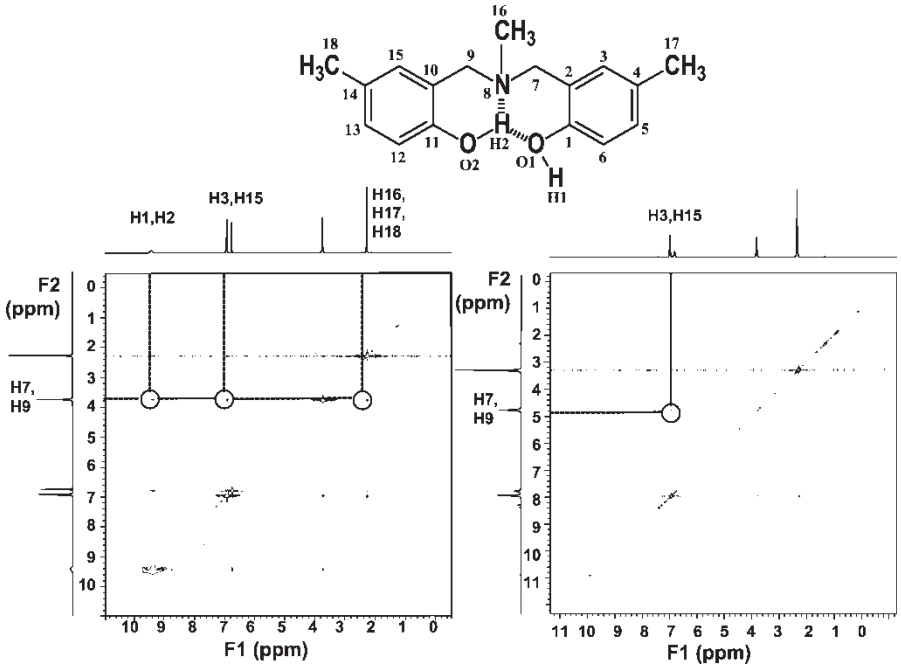

FIGURE 10 $^1H-^1H$ NOESY spectra of (a) **1** and (b) **1**–$CuCl_2$ in $CDCl_3$.

while the interaction with metal ions was dominant. The peak resulting from the interaction of the methylene protons (H7, H9) with the methyl protons (H16) disappeared whereas that of the methylene protons (H7, H9) with the aromatic protons (H3, H15) became weaker, implying the effect of the metal ion on **1** during host–guest formation.

Inclusion Compounds of *N,N*-bis-(2-hydroxybenzyl)alkylamine Derivatives with other Transition Metal Ions

Another question of interest was to what extent a different transition metal *d*-orbital system would affect the inclusion phenomena. For example, the successful inclusion phenomena of Cu^{2+} ($3d^9$) might be due to an empty 4s orbital being available to accept electrons from *N,N*-bis(2-hydroxybenzyl) alkylamine derivatives. A study of the formation of complexes of **1** with other transition metal ions was therefore carried out.

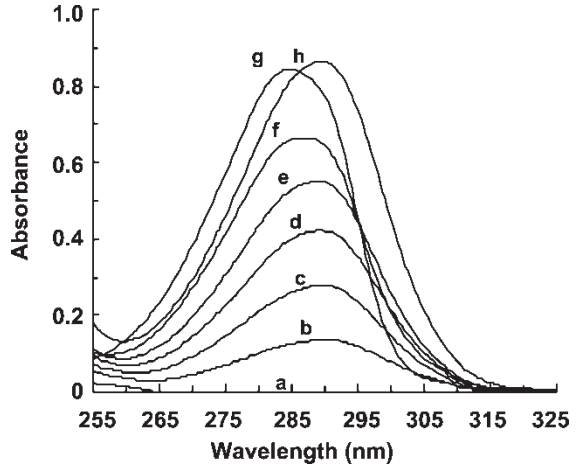

FIGURE 11 UV Spectra of **1** (1.65×10^{-4} M) mixed with $ZnCl_2$ (1.65×10^{-4} M) in methanol at the volumetric ratios of a) 0:6, b) 1:5, c) 2:4, d) 3:3, e) 4:2, f) 5:1 and g) 6:0, and h) 1.65×10^{-4} M solution of **1** mixed with $ZnCl_2$ at the molar ratio of 1:8.

Figure 11 shows UV-Vis spectra of solutions of **1** with zinc ions in methanol with ratios of 1:5 to 5:1. In methanol, **1** gives a peak maximum at 284 nm (Fig. 11(g)) whereas $ZnCl_2$ does not show any peak (Fig. 11(a)) over the range 255–325 nm. This is different from the $CuCl_2$ system since there is no new peak from the solution of $ZnCl_2$ and **1** but a bathochromic effect. For example, in the case of **1**–$ZnCl_2$ for 1:5, the peak is shifted from 284 to 290 nm, implying a host–guest system. A saturated system of $ZnCl_2$–**1** shows a significant peak at 290 nm (Fig. 11(h)). This implies that the high concentration of $ZnCl_2$ increases the metal ion interaction with the host molecules resulting in a hyperchromic effect. Considering the peaks b–f, the apparent peak shift might come from the overlap of the two peaks, i.e. 284 nm (due to the host) and 290 nm (due to the host–guest complex).

^1H NMR measurements were also undertaken to confirm inclusion of Zn^{2+} with **1.** Considering the electronic orbital of Zn^{2+}, we speculate that the fully filled $3d^{10}$ orbital with no available *s*-orbital might prevent electron sharing with **1**. A series of spectra of **1**–$ZnCl_2$ show all protons deshielded similar to **1**–$CuCl_2$ (Figs. 2 and 12(c)–(e)). The methylene peak shows only

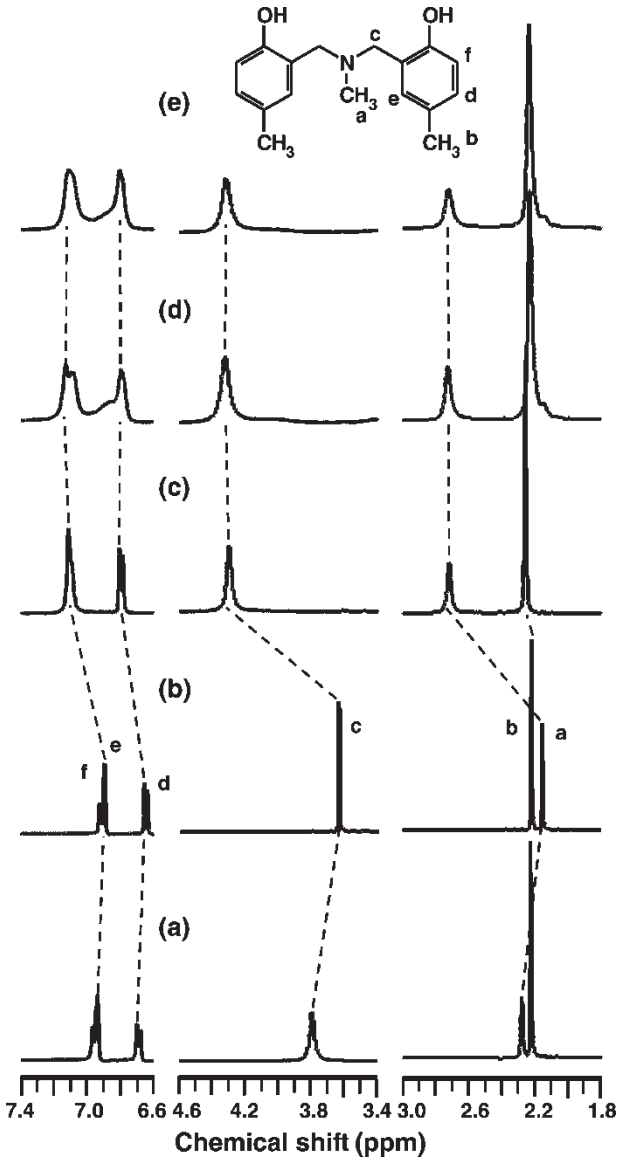

FIGURE 12 ^{1}H NMR spectra of (a) **1**–$CdCl_2$, (b) **1** and **1**–$ZnCl_2$ at the ratios of (c) 1:1, (d) 1:8 and (e) 1:15 in methanol-d_4.

peak shifting without splitting. This implies that the Zn^{2+} maintains the equivalent structure of the two $-CH_2-$ groups (adjacent to the N atom) even upon host–guest formation. In other words, the fully filled *d*-orbital in Zn^{2+} might obstruct the sharing of the lone pair electrons of OH and N in the host–guest compound. When the ratio of **1**–$ZnCl_2$ was as high as 1:8 or 1:15, the aromatic peaks were significantly broad. This suggests that there are various averaging aromatic proton environments in the inclusion complex formed between **1** and $ZnCl_2$.

In order to confirm the electronic orbital involved in the inclusion process, $CdCl_2$ was also studied. We expected that $CdCl_2$ with the outer orbital $5s^2$ would show similar results to $ZnCl_2$.

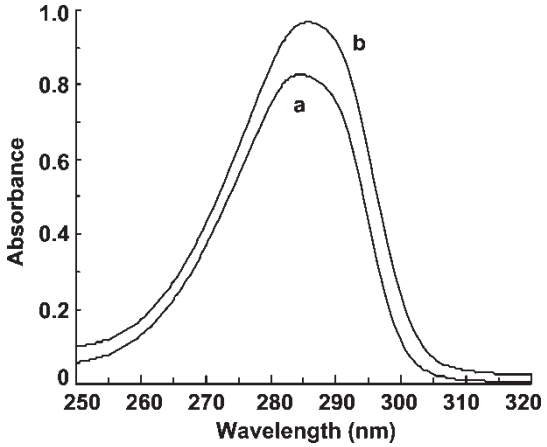

FIGURE 13 UV Spectra of (a) 1.65×10^{-4} M solution of **1** and (b) **1**–$CdCl_2$ (1:8).

The mixing of a solution of **1** with $CdCl_2$ was observed by UV (Fig. 13) and gave a peak with a hyperchromic shift similar to that of $ZnCl_2$, implying that inclusion had occurred. The ^{1}H NMR spectrum of **1**–$CdCl_2$ shows a shift in the methylene protons but the change is small compared to that of **1**–$ZnCl_2$ (Fig. 12(a)). This implies a difficulty in interaction with the host. The small changes in ^{1}H NMR and UV also imply that the size of the metal ions also has an effect on complexation.

CONCLUSION

The present work clarifies the inclusion compound of *N*,*N*-bis(2-hydroxybenzyl)alkylamines with transition metals by using copper, cadmium and zinc as model ions. In solution, the host–guest ratios of *N*,*N*-bis(2-hydroxybenzyl)alkylamine derivatives with $CuCl_2$ were found to be 2:1. Although the host–guest formation is dependent on the structure of the host, the interaction might form at the hydroxyl and aza-methylene group as suggested from UV-Vis, ^{1}H NMR and ^{1}H–^{1}H NOESY. The ESIMS showed cluster patterns indicating inclusion phenomena by the molecular assembly of *N*,*N*-bis(2-hydroxybenzyl)-alkylamines. The studies on the interaction with metal ions in various solvents suggested that the inclusion might be enhanced by either hydrogen bonding or polar–polar interaction. For the solid-state host–guest compound, the DSC clarified that the *N*,*N*-bis(2-hydroxybenzyl)alkylamine derivatives lost some thermal stability after forming inclusion compounds with metal ions. Overall, we found that with respect to the nature of *N*,*N*-bis-(2-hydroxybenzyl)alkylamine derivatives, the larger the bulky group at the aza position is, the lower the metal ion acceptance of the host will be, whereas with regard to the transition metals, the vacant electron orbital was an important factor for inclusion.

EXPERIMENTAL

Chemicals

Paraformaldehyde, methylamine, 4-ethylphenol, 2,4-dimethylphenol, and anhydrous sodium sulfate were purchased from Fluka, Switzerland. *p*-Cresol, propylamine, cyclohexylamine, and methanol-d_4 were obtained from Merck, Germany. Sodium hydroxide and isopropanol were provided from Carlo Erba, Italy. Copper(II) chloride and zinc(II) chloride were purchased from Shimakyu's Pure Chemicals, Japan, and Ajax Finechem, Australia, respectively. 1,4-Dioxane, diethyl ether, isopropanol, dichloromethane, and *N*,*N*-dimethylsulfoxide (DMSO) were from Labscan, Ireland. Chloroform-*d*, and methyl sulfoxide-d_6 (DMSO-d_6) were purchased from Aldrich, Germany. All chemicals were used without further purification.

Instruments

Fourier transform infrared spectra (FTIR) were recorded in Nujol in the range 4000–400 cm^{-1} with 64 scans at a resolution of 2 cm^{-1} on a Bruker Equinox55/S spectrophotometer using a deuterated triglycinesulfate detector (DTGS) with a specific detectivity, D^*, of 1×10^9 cm $Hz^{1/2}$ w^{-1}. Differential scanning calorimetry analysis (DSC) was carried out by a Perkin Elmer DSC7 from 50°C to 200°C at a heating rate of 10°C/min. X-ray diffraction (XRD) patterns were obtained from a Rigaku RINT 2000, using CuK_α ($\lambda = 0.154$ nm) as an X-ray source with 2θ of 5–50° operating at 40 kV and 30 mA with Ni filter. Proton nuclear magnetic resonance (^{1}H NMR) spectra and two-dimensional nuclear Overhauser enhancement (^{1}H–^{1}H NOESY) spectra were obtained using a Varian Mercury-400BB spectrometer. The host–guest ratio was studied by electrospray ionization mass spectrometry (ESIMS), using a PE SCIEX API III Biomolecular Mass Analyzer. UV-Vis absorbance data were obtained on a Perkin Elmer UV-VIS spectrometer Lambda 16.

Synthesis

A series of the derivatives, i.e., *N*,*N*-bis-(2-hydroxy-5-methylbenzyl)methylamine, **1**, *N*,*N*-bis(2-hydroxy-5-methylbenzyl)propylamine, **2**, *N*,*N*-bis(2-hydroxy-5-methylbenzyl)cyclohexylamine, **3**, *N*,*N*-bis(2-hydroxy-5-ethylbenzyl)methylamine, **4**, and *N*,*N*-bis(2-hydroxy-3,5-dimethylbenzyl)methylamine, **5**, were prepared from a ring-opening reaction of the relevant benzoxazine and phenol derivatives. Mixtures of 3,4-dihydro-3,6-dimethyl-2H-1,3-benzoxazine and *p*-cresol (1:1) were prepared and stirred at 60°C. The mixtures were allowed to react until viscous and left for precipitation. The precipitates obtained were collected, and washed with diethyl ether before vacuum drying. The compounds were recrystallized in chloroform before use. Similarly, 3,4-dihydro-6-methyl-3-propyl-2H-1,3-benzoxazine, 3,4-dihydro-6-methyl-3-cyclohexyl-2H-1,3-benzoxazine, 3,4-dihydro-6-ethyl-3-methyl-2H-1,3-benzoxazine, and 3,4-dihydro-3,6,8-trimethyl-2H-1,3-benzoxazine were reacted with *p*-cresol, *p*-cresol, 4-ethylphenol, and 2,4-dimethylphenol, respectively. The compounds obtained were qualitatively analyzed by FTIR, ^{1}H NMR and EA.

***N*,*N*-bis(2-hydroxy-5-methylbenzyl)methylamine (1)**: 90% yield; $R_f = 0.24$ (5% MeOH in $CHCl_3$); clear and colorless solid; mp = 163°C; FTIR (KBr, cm^{-1}): 3271 (br, OH), 1499 (vs, C–C), 1456 (m, N–CH_3), 1249 (s, C–N), 1209 (m, C–N–C), 815 (vs, C–N–C); ^{1}H NMR (200 MHz, $CDCl_3$, ppm): δ_H 2.23 (6H, s, Ar–**CH_3**), 2.23 (3H, s, N–**CH_3**), 3.69 (4H, s, Ar–**CH_2**–N), 6.70 (2H, d, Ar–**H**), 6.83 (2H, s, Ar–**H**), 6.86 (2H, d, Ar–**H**). Anal.calcd. for $C_{17}H_{21}NO_2$: C, 75.28; H, 7.75; and N, 5.17. Found: C, 75.31; H, 7.77; and N, 5.19%.

***N*,*N*-bis(2-hydroxy-5-methylbenzyl)propylamine (2)**: 80% yield; $R_f = 0.22$ (5% MeOH in $CHCl_3$); clear and colorless solid; mp = 149°C; FTIR (KBr, cm^{-1}): 3251 (br, OH), 1501 (vs, C–C), 1467 (m, N–CH_3), 1276 (s, C–N), 1210 (s, C–N–C), 819 (s, C–N–C); ^{1}H NMR (200 MHz, $CDCl_3$, ppm): δ_H 0.87 (3H, t, **CH_3**–CH_2–CH_2–N), 1.65 (2H, m, CH_3–**CH_2**–CH_2–N), 2.22 (6H, s, Ar–**CH_3**), 2.50 (2H, t, CH_3–CH_2–**CH_2**–N), 3.70 (4H, s, Ar–**CH_2**–N), 6.68 (2H, d, Ar–**H**), 6.85 (2H, s, Ar–**H**), 6.90 (2H, d, Ar–**H**). Anal.calcd. for $C_{19}H_{25}NO_2$: C, 76.25; H, 8.36; and N, 4.69. Found: C, 76.28; H, 8.31; and N, 4.70%.

***N*,*N*-bis(2-hydroxy-5-methylbenzyl)cyclohexylamine (3)**: 80% yield; $R_f = 0.30$ (5% MeOH in $CHCl_3$); clear and colorless solid; mp = 181°C; FTIR (KBr, cm^{-1}): 3226 (br, OH), 1500 (vs, C–C), 1449 (m, N–CH), 1249 (s, C–N), 1210 (m, C–N–C), 819 (s, C–N–C); ^{1}H NMR (200 MHz, $CDCl_3$, ppm): δ_H 1.1 (2H, m, **CH_2**), 1.45 (4H, m, **CH_2**), 1.82 (4H, m, **CH_2**), 2.22 (6H, s, **CH_3**–Ar), 2.70 (1H, m, **CH**), 3.72 (4H, s, Ar–**CH_2**–N), 6.68 (2H, d, Ar–**H**), 6.85 (2H, s, Ar–**H**), 6.90 (2H, d, Ar–**H**). Anal.calcd. for $C_{22}H_{29}NO_2$: C, 77.88; H, 8.55; and N, 4.13. Found: C, 77.90; H, 8.56; and N, 4.16%.

***N*,*N*-bis(2-hydroxy-5-ethylbenzyl)methylamine (4)**: 90% yield; $R_f = 0.34$ (5% MeOH in $CHCl_3$); clear and colorless solid; mp = 130°C; FTIR (KBr, cm^{-1}): 3301 (br, OH), 1499 (vs, C–C), 1460 (m, N–CH_3), 1251 (s, C–N), 1207 (m, C–N–C), 821 (s, C–N–C); ^{1}H NMR (200 MHz, $CDCl_3$, ppm): δ_H 1.17 (6H, t, Ar–CH_2–**CH_3**), 2.25 (3H, s, N–**CH_3**), 2.54 (4H, q, Ar–**CH_2**–CH_3), 3.72 (4H, s, Ar–**CH_2**–N), 6.73 (2H, d, Ar–**H**), 6.87 (2H, s, Ar–**H**), 6.94 (2H, d, Ar–**H**). Anal.calcd. for

$C_{19}H_{25}NO_2$: C, 76.26; H, 8.36; and N, 4.68. Found: C, 76.24; H, 8.35; and N, 4.65%.

***N,N*-bis(2-hydroxy-3,5-dimethylbenzyl)methylamine (5)**: 80% yield; $R_f = 0.39$ (5% MeOH in $CHCl_3$); clear and colorless solid; mp = 123°C; FTIR (KBr, cm^{-1}): 3399 (br, OH), 1484 (vs, C–C), 1427 (m, N–CH_3), 1243 (m, C–N), 1214 and 1201 (m, C–N–C), 847 (m, C–N–C); ^1H NMR (200 MHz, $CDCl_3$, ppm): δ_H 2.22 (12H, s, Ar–**CH_3**), 2.25 (3H, s, N–**CH_3**), 3.68 (4H, s, Ar–**CH_2**–N), 6.72 (2H, s, Ar–**H**), 6.81 (2H, s, Ar–**H**). Anal.calcd. for $C_{19}H_{25}NO_2$: C, 76.26; H, 8.36; and N, 4.68. Found: C, 76.27; H, 8.34; and N, 4.69%.

Complexation in Solution

Methanolic solutions of each derivative and copper chloride (1.65×10^{-4} M) were made up and the two solutions were mixed in the following ratios: (**1**–**5**)-copper chloride, 1:5, 2:4, 3:3, 4:2, and 5:1, respectively. The mixtures were shaken vigorously for 1 min and left for 12 h, UV-Vis absorbance at the maximum peak position was measured and plotted as Job's plot. Zinc chloride was also used instead of copper chloride. Each chloride salt of copper, zinc, and cadmium was mixed with the *N,N*-bis(2-hydroxybenzyl)alkylamine derivatives to give a 1:1 molar ratio, and dissolved in methanol-d_4 for analysis by ^1H NMR. Similarly, DMSO-d_6 and $CDCl_3$ were used as solvents to study the solvent effect.

Solid State of Host–metal Ion Complex

Solutions of *N,N*-bis(2-hydroxybenzyl)alkylamine derivatives in chloroform (7×10^{-3}M) and copper chloride in deionized water (0.7 M) were prepared, vigorously mixed and left for 3d. The organic phase was collected, dried by anhydrous Na_2SO_4, and evaporated to obtain a green powder, which was characterized by FTIR, DSC, and XRD. The concentration of copper chloride in the aqueous phase was determined (to establish the host–guest ratio) by UV-Vis spectroscopy. The powder was dissolved in $CDCl_3$ for analysis by ^1H–^1H NOESY NMR.

Percentage Metal Ion Extraction

Solutions of copper chloride in deionized water (2.5×10^{-2} M) and the *N,N*-bis(2-hydroxybenzyl)alkylamine derivatives in chloroform (0.1, 7.5×10^{-2}, 5.0×10^{-2}, 2.5×10^{-2}, 1.25×10^{-2}, 6.25×10^{-3}, and 2.5×10^{-4} M) were prepared; 5 ml of each solution were mixed together, vigorously shaken for 1 min, and left overnight. The absorbance at 815 nm was measured and calculated for percentage extraction by the equation $[(A_0 - A)/A_0] \times 100$ where A_0 is the initial absorbance, and A is the absorbance after extraction with the *N,N*-bis(2-hydroxybenzyl)alkylamine derivative.

Acknowledgements

The authors (S.P., S.C.) acknowledge the financial support from the Thailand Research Fund through the Royal Golden Jubilee Ph.D. Program (Grant No. PHD/0189/2544). The authors would like to thank Prof. Mikiji Miyata, Department of Material and Life Science, Graduate School of Engineering, Osaka University, for arranging the scholarship from Academic Frontiers Student Exchange Promotion Program. The appreciation is extended to Prof. Kohji Tashiro, Department of Macromolecular Science, Graduate School of Science, Osaka University, for valuable suggestions throughout the work.

References

[1] Pedersen, C. J. *J. Am. Chem. Soc.* **1967**, *89*, 7017.
[2] Pedersen, C. J.; Frensdroff, H. K. *Angew. Chem. Int. Ed. Engl.* **1972**, *11*, 16.
[3] Lehn, J.-M. In *Nobel Lectures in Chemistry (1981–1990)*; Frangsmyr, T. and Malmstrom, B. G., Eds.; World Scientific: Singapore, 1992; p 444.
[4] Tummler, B.; Maass, G.; Weber, E.; Wehner, W.; Vogtle, F. *J. Am. Chem. Soc.* **1977**, *99*, 4683.
[5] Ardini, A.; Pochini, A.; Reverberi, S.; Ungaro, R. *Tetrahedron* **1986**, *42*, 2089.
[6] Knight, D. A.; Kim, V.; Butcher, R. J.; Harper, B. A.; Schull, T. L. *J. Chem. Soc., Dalton Trans.* **2002**, 824.
[7] Yasuda, S.; Miyake, K.; Sumaoka, J.; Komiyama, M.; Shigekawa, H. *Jpn. J. Appl. Phys.* **1999**, *38*, 3888.
[8] Min, K. S.; Suh, M. P. *Eur. J. Inorg. Chem.* **2001**, *2*, 449.
[9] Raymo, F. M.; Bartberger, M. D.; Houk, K. N.; Stoddart, J. F. *J. Am. Chem. Soc.* **2001**, *123*, 9264.
[10] Ning, X.; Ishida, H. *J. Polym. Sci., Part A: Polym. Chem.* **1994**, *32*, 1121.
[11] Chirachanchai, S.; Laobuthee, A.; Phongtamrug, S.; Siripatanasarakit, W.; Ishida, H. *J. Appl. Polym. Sci.* **2000**, *77*, 2561.
[12] Laobuthee, A., Dissertation, Chulalongkorn University, Bangkok, Thailand.
[13] Laobuthee, A.; Chirachanchai, S.; Ishida, H.; Tashiro, K. *J. Am. Chem. Soc.* **2001**, *123*, 9947.
[14] Laobuthee, A.; Chirachanchai, S. *Chem. Lett.* **2002**, *31*, 614.
[15] Chirachanchai, S.; Phongtamrug, S.; Laobuthee, A. *Chem. Lett.* **2003**, *32*, 432.
[16] Laobuthee, A.; Ishida, H.; Chirachanchai, S. *J. Incl. Phenom. Macro.* **2003**, *47*, 179.
[17] Makarska, M.; Radzki, St.; Legendziewicz, J. *J. Alloy. Compd.* **2002**, *341*, 233.
[18] Yamagishi, T.; Tani, K.; Ishida, S.; Nakamoto, Y. *Polym. Bull.* **1994**, *33*, 281.
[19] Miyata, M.; Shibakami, M.; Chirachanchai, S.; Takemoto, K.; Kasai, N.; Miki, K. *Nature* **1990**, *343*, 446.
[20] Ganem, B.; Li, Y.-T.; Henion, J. D. *J. Am. Chem. Soc.* **1991**, *113*, 6294.
[21] Lippmann, T.; Wilde, H.; Pink, M.; Schafer, A.; Hesse, M.; Mann, G. *Angew. Chem. Int. Ed. Engl.* **1993**, *32*, 1195.
[22] Selva, A.; Redenti, E.; Zanol, M.; Ventura, P.; Casetta, B. *Org. Mass Spectrom.* **1993**, *28*, 983.
[23] Haskins, N. J.; Saunders, M. R.; Camilleri, P. *Rapid Commun. Mass Spectrom.* **1994**, *8*, 423.
[24] Rossel, C. P.; Carreno, J. S.; Rodriguez-Baeza, M.; Alderete, J. B. *Quim. Nova* **2000**, *23*, 749.
[25] Sanders, J. K. M.; Hunter, B. K. *Modern NMR Spectroscopy: A Guide for Chemists*; Oxford University Press: New York, 1987; pp 163–172.